



Synthesis and structure of a 1:1 cocrystal of *N,N'*-bis(pyridin-3-ylmethyl)pyromellitic diimide and naphthalene-2,6-dicarboxylic acid

Luccile Mbonzhe and Eustina Batisai*

University of Venda, P Bag X5050, Thohoyandou, 0950, South Africa. *Correspondence e-mail: Eustina.Batisai@univen.ac.za

Received 14 May 2026

Accepted 11 June 2026

Edited by W. T. A. Harrison, University of Aberdeen, United Kingdom

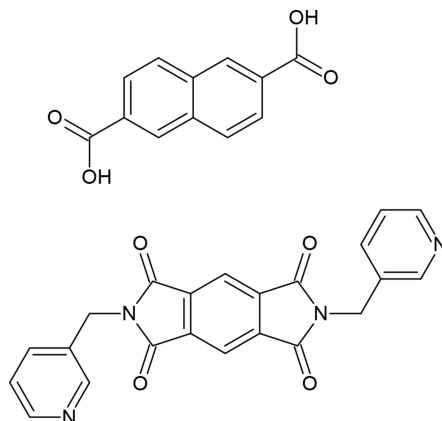
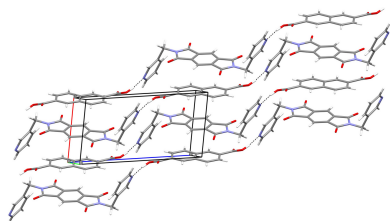
Keywords: cocrystal; pyromellitic diimide; Hirshfeld surface analysis; naphthalenedicarboxylic acid.**CCDC reference:** 2561484**Supporting information:** this article has supporting information at journals.iucr.org/e

In the title cocrystal, $C_{22}H_{14}N_4O_4 \cdot C_{12}H_8O_4$, both components are completed by crystallographic inversion symmetry and the dihedral angle between the central fused ring system and the pendant pyridine ring is $66.21(5)^\circ$. In the extended structure, the components are linked by $O-H \cdots N$ hydrogen bonds, generating [001] chains, and the packing is consolidated by $\pi-\pi$ stacking and $C-H \cdots O$ interactions.

1. Chemical context

N,N'-Bis(pyridin-3-ylmethyl)pyromellitic diimide, $C_{22}H_{14}N_4O_4$, (Lig1) consists of a pyromellitic diimide core linked to *meta*-substituted pyridyl groups *via* $-CH_2-$ linkages. These rotatable linkages impart conformational flexibility, allowing Lig1 to adopt Z_C and Z_T modes, where Z denotes an *anti* orientation of the pyridyl rings, while C (*cis*) and T (*trans*) describe the relative positions of the pyridyl nitrogen atoms (Yan *et al.*, 2010). The pyromellitic diimide core further promotes $\pi-\pi$ stacking interactions, contributing to supramolecular assembly. Owing to its semi-rigid nature, Lig1 has been widely employed in the construction of metal-organic frameworks (MOFs) exhibiting diverse topologies, with potential applications in gas sorption (Li *et al.*, 2012) and fluorescence (Huang *et al.*, 2020; Li *et al.*, 2018).

Deprotonated naphthalene dicarboxylic acid ($C_{12}H_8O_4$; NDC) ligands are also widely used to prepare MOFs with potential applications in gas storage, gas separation, luminescence and catalysis (Gangu *et al.*, 2017). Their aromatic ring system allows for increased $\pi-\pi$ stacking interactions, enhancing supramolecular recognition and enabling the formation of complex polymer networks.



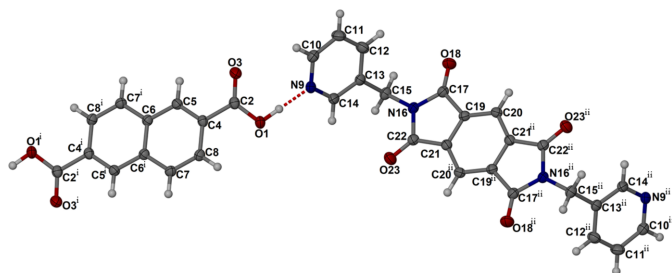


Figure 1

The molecular structure of (**I**) with displacement ellipsoids drawn at the 70% probability level. [Symmetry codes: (i) $2 - x, 1 - y, 2 - z$; (ii) $1 - x, 1 - y, -z$].

The aim of this work was to prepare a zinc mixed-ligand MOF containing Lig1 and NDC. However, single-crystal X-ray diffraction (SCXRD) revealed that a 1:1 cocrystal of Lig1 and NDC, (**I**), had formed from the solvothermal reaction and we now describe its structure.

2. Structural commentary

Compound (**I**) crystallizes in the triclinic space group $P\bar{1}$ with half a molecule of Lig1 and half a molecule of NDC in the asymmetric unit (Fig. 1). Both complete molecules are generated by crystallographic inversion centres at $(1/2, 1/2, 0)$ and $(1, 1/2, 1)$ for the asymmetric atoms of Lig1 and NDC, respectively. The Lig1 molecule adopts a Z_T mode and the dihedral angle between the central fused ring system and the pendant pyridine ring is $66.21(5)^\circ$.

3. Supramolecular features

In the extended structure of (**I**), the NDC molecule links to Lig1 *via* an $O1-H1\cdots N9$ hydrogen bond between the carboxylic acid group of NDC and the py-*N* of Lig1, and a secondary interaction between the Ar-H atom of Lig1 and the $C=O$ group of the NDC molecule ($C10-H10\cdots O3$). These interactions result in extended chains of alternating Lig1 and

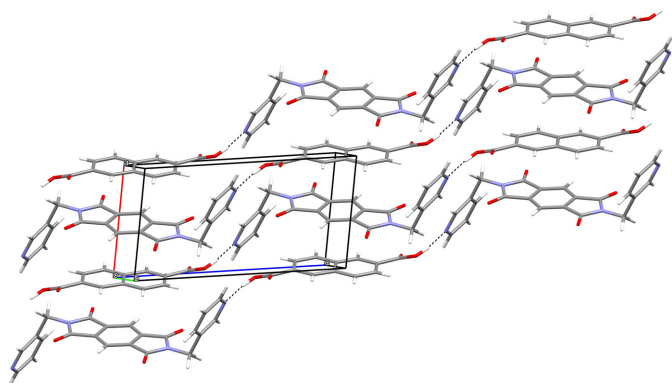


Figure 2

The packing of (**I**) viewed down the *b*-axis direction.

Table 1

Hydrogen-bond geometry ($\text{\AA}, ^\circ$).

$D-H\cdots A$	$D-H$	$H\cdots A$	$D\cdots A$	$D-H\cdots A$
$O1-H1\cdots N9$	0.95 (1)	1.64 (1)	2.5806 (13)	172 (2)
$C15-H15A\cdots O3^i$	0.99	2.56	3.4073 (14)	143
$C11-H11\cdots O23^{ii}$	0.95	2.51	3.2402 (15)	134
$C10-H10\cdots O3^{iii}$	0.95	2.64	3.2414 (15)	122
$C11-H11\cdots O3^{iii}$	0.95	2.62	3.2207 (15)	122

Symmetry codes: (i) $-x + 1, -y + 2, -z + 1$; (ii) $x, y + 1, z$; (iii) $-x + 2, -y + 2, -z + 1$.

NDC molecules running along the crystallographic *c*-axis direction (Table 1, Fig. 2).

The chains stack in the *ac* plane in an offset arrangement facilitated by $\pi-\pi$ stacking interactions [centroid-to-centroid distance = $3.767(1) \text{\AA}$] between the pyridyl moieties of Lig1 of adjacent chains, as well as $\pi-\pi$ interactions [centroid-to-centroid distance = $3.761(1) \text{\AA}$] between the pyromellitic moiety of Lig1 and the naphthalene moiety of NDC of adjacent chains. Additionally, the chains interact with neighboring chains *via* $C-H\cdots O$ interactions in the *ac* plane ($C15-H15A\cdots O3$) as well as in the *b*-axis direction ($C11-H11\cdots O23$) (Fig. 2).

4. Hirshfeld surface analysis

To further quantify the nature and relative contributions of intermolecular interactions within the crystal structure of (**I**), two-dimensional fingerprint plots were generated using *CrystalExplorer* (Spackman *et al.* 2021). The Hirshfeld surface was constructed from a hydrogen-bonded unit comprising one NDC and one Lig1 molecule. The breakdown of intermolecular contacts and their percentage contributions to the total Hirshfeld surface are presented in Fig. 3. The contributions follow the order $O\cdots H/H\cdots O$ (32%) > $H\cdots H$ (29%) > $C\cdots C$ (14%) > $C\cdots H/H\cdots C$ (13%) > $N\cdots H/H\cdots N$ (5%) > $C\cdots O/O\cdots C$ (2.9%). Although $O\cdots H/H\cdots O$ interactions make the largest contribution to the Hirshfeld surface, these contacts are relatively long, with the closest atom-atom distance of approximately 2.3\AA , and are mainly associated

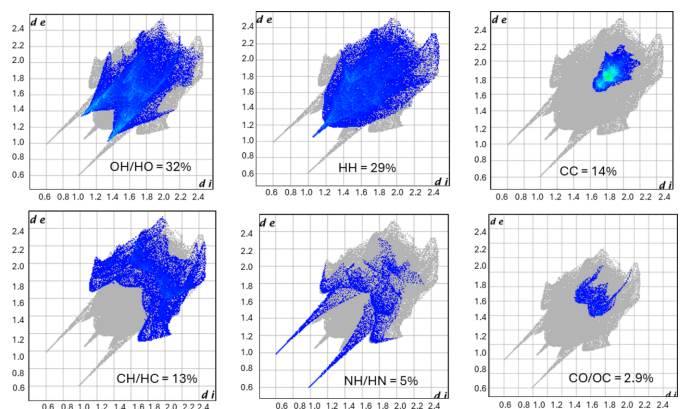


Figure 3

Two-dimensional fingerprint plots for (**I**) showing the various contributions to the Hirshfeld surface.

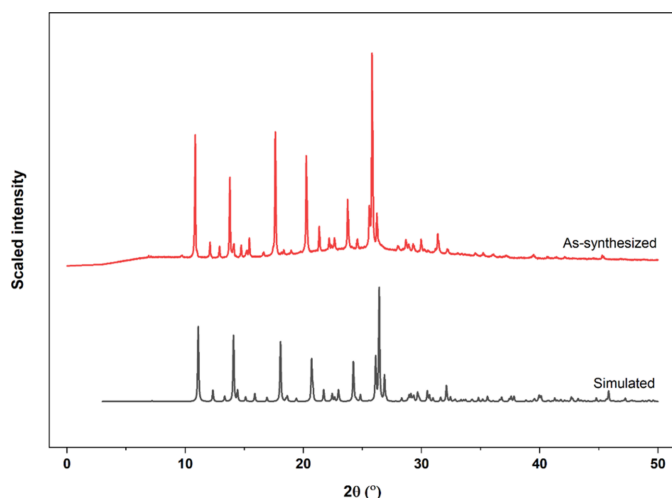


Figure 4
Experimental PXRD pattern of **(I)** (red) overlaid with the simulated pattern generated from SCXRD data (black), confirming phase purity.

with weaker C–H···O interactions. H···H contacts also contribute significantly, indicating that van der Waals interactions play an important role in consolidating the crystal structure. The C···C and C···H interactions contribute 14% and 13%, respectively, and can be attributed to π – π stacking and C–H··· π interactions. N···H/H···N interactions, associated with O–H···N hydrogen bonding, contribute a smaller proportion (5%) but represent the shortest intermolecular contacts, with a closest atom–atom distance of approximately 1.6 Å.

5. Thermogravimetric analysis (TGA) and powder X-ray diffraction (PXRD)

PXRD analysis was performed to assess the bulk phase purity of **(I)**. A comparison of the PXRD pattern of the as-synthesized sample with the simulated pattern of **(I)** shows good agreement, which indicates phase purity of the sample (Fig. 4). The TGA curve shows that the cocrystal decomposes at 290 °C (Fig. 5).

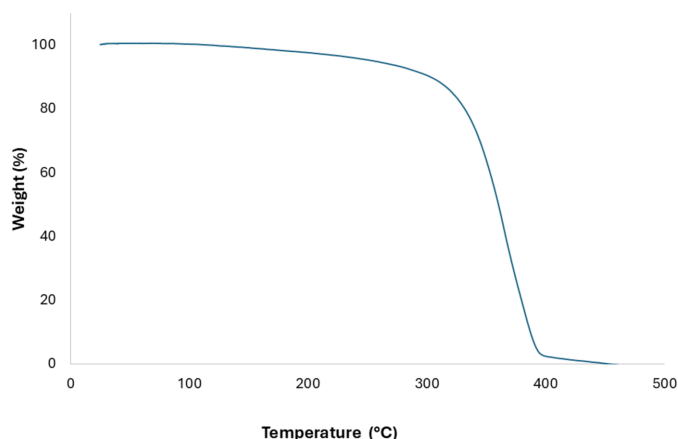


Figure 5
TGA curve of **(I)**. Decomposition starts at 290 °C.

Table 2
Experimental details.

Crystal data	
Chemical formula	C ₂₂ H ₁₄ N ₄ O ₄ ·C ₁₂ H ₈ O ₄
<i>M_r</i>	614.55
Crystal system, space group	Triclinic, <i>P</i> $\bar{1}$
Temperature (K)	130
<i>a</i> , <i>b</i> , <i>c</i> (Å)	6.9314 (2), 8.3554 (3), 12.5463 (4)
α , β , γ (°)	79.716 (1), 80.977 (1), 74.432 (1)
<i>V</i> (Å ³)	684.15 (4)
<i>Z</i>	1
Radiation type	Mo <i>K</i> α
μ (mm ^{−1})	0.11
Crystal size (mm)	0.28 × 0.17 × 0.13
Data collection	
Diffractometer	BRUKER D8 QUEST
Absorption correction	Multi-scan (<i>SADABS</i> ; Krause <i>et al.</i> , 2015)
<i>T_{min}</i> , <i>T_{max}</i>	0.650, 0.746
No. of measured, independent and observed [<i>I</i> > 2 σ (<i>I</i>)] reflections	23721, 3391, 3048
<i>R_{int}</i>	0.040
(<i>sin</i> θ / λ) _{max} (Å ^{−1})	0.667
Refinement	
<i>R</i> [<i>F</i> ² > 2 σ (<i>F</i> ²)], <i>wR</i> (<i>F</i> ²), <i>S</i>	0.039, 0.107, 1.10
No. of reflections	3391
No. of parameters	211
No. of restraints	1
H-atom treatment	H atoms treated by a mixture of independent and constrained refinement
$\Delta\rho_{\max}$, $\Delta\rho_{\min}$ (e Å ^{−3})	0.36, −0.28

Computer programs: *APEX4* and *SAINT* (Bruker, 2022), *SHELXT* (Sheldrick, 2015a), *SHELXL2019/3* (Sheldrick, 2015b) and *X-SEED* (Barbour, 2020).

6. Database survey

A search of the Cambridge Structural Database (CSD) (Groom *et al.*, 2016) showed that Lig1 has been used mostly in the preparation of coordination complexes. Of the 20 crystal structures deposited Co [DIBBAU, DIBBEY, DIBBIC (Li *et al.*, 2018), OWEYEV (Li *et al.*, 2011)], Zn [OWEYUL (Li *et al.*, 2011), FISCEQ (Lü *et al.* 2005b), PALYIL (Lü *et al.* 2005a)], Cd [FISCAM (Lü *et al.* 2005b), PADHOT (Chai *et al.* 2010), PALYUX (Lü *et al.* 2005a), ZAVQIZ (Li *et al.*, 2017), ZAXSOI (Li *et al.*, 2012)], Ag [QAHBEI, QAHBIM; Yan *et al.*, 2011], Hg [HUHZUI (Huang *et al.*, 2020), PEVYUL (Li *et al.*, 2007)], Ni (HUJBAS; Huang *et al.*, 2020) and Mn [OWEXO (Li *et al.*, 2011), ZAVQEV Li *et al.*, 2017)] and one entry is a salt of protonated Lig1 and a perchlorate ion (FISBUF; Lü *et al.*, 2005). The coordination complexes exhibit structural diversity, with some investigated for CO₂ sorption (Li *et al.*, 2012) and fluorescence properties (Huang *et al.*, 2020; Li *et al.*, 2018). A search on the CSD for NDC produced 683 coordination complexes containing NDC either by itself or in combination with other ligands. Additionally, there are 40 hits where NDC features in cocrystals or salts.

7. Synthesis and crystallization

Lig1 was synthesized according to a reported procedure (Li *et al.* 2009). Compound **(I)** crystallized from a solvothermal reaction of Lig1 (10 mg, 0.025 mmol), NDC (16 mg,

0.074 mmol), and $\text{Zn}(\text{NO}_3)_2 \cdot 6\text{H}_2\text{O}$ (20 mg, 0.067 mmol) in 3 ml of *N,N*-dimethylformamide (DMF) at 373 K. Cream crystals of (**I**) formed after 3 days. The vial was then removed from the oven and washed with 2 ml of DMF.

8. Refinement

Crystal data, data collection and structure refinement details are summarized in Table 2. C-bound H atoms were positioned ($\text{C}-\text{H} = 0.95\text{--}0.99 \text{ \AA}$) geometrically and refined as riding $U_{\text{iso}}(\text{H}) = 1.2U_{\text{eq}}(\text{C})$. The OH H atom was found in a difference map and refined with $U_{\text{iso}}(\text{H}) = 1.5U_{\text{eq}}(\text{O})$.

Acknowledgements

EB thanks the National Research Foundation of South Africa for financial support. LM thanks the NRF and SASOL Foundation for a bursary.

Funding information

Funding for this research was provided by: National Research Foundation of South Africa (grant Nos. 129759, 138178).

References

- Barbour, L. J. (2020). *J. Appl. Cryst.* **53**, 1141–1146.
- Bruker (2022). *APEX4* and *SAINT*. Bruker AXS Inc., Madison, Wisconsin, USA.
- Chai, W., Lü, X., Bi, W., Song, J. & Kang, B. (2010). *J. Chem. Crystallogr.* **40**, 740–745.
- Gangu, K. K., Maddila, S. & Jonnalagadda, S. B. (2017). *Inorg. Chim. Acta* **466**, 308–323.
- Groom, C. R., Bruno, I. J., Lightfoot, M. P. & Ward, S. C. (2016). *Acta Cryst.* **B72**, 171–179.
- Huang, X. M., Li, G. B., Pan, R.-K. & Liu, S. G. (2020). *Transit. Met. Chem.* **45**, 187–193.
- Krause, L., Herbst-Irmer, R., Sheldrick, G. M. & Stalke, D. (2015). *J. Appl. Cryst.* **48**, 3–10.
- Li, X., Fan, X. & Zeng, Q. (2007). *Int. J. Mol. Sci.* **8**, 29–41.
- Li, G. B., He, J.-R., Pan, M., Deng, H. Y., Liu, J.-M. & Su, C. Y. (2012). *Dalton Trans.* **41**, 4626–4633.
- Li, G. B., Liu, J. M., Cai, Y. P. & Su, C. Y. (2011). *Cryst. Growth Des.* **11**, 2763–2772.
- Li, G. B., Liu, J. M., Yu, Z. Q., Wang, W. & Su, C. Y. (2009). *Inorg. Chem.* **48**, 8659–8661.
- Li, G. B., Pan, R. K. & Liu, S. G. (2017). *Spectrochim. Acta A Mol. Biomol. Spectrosc.* **187**, 168–173.
- Li, G. B., Yang, Q. Y., Pan, R. K. & Liu, S. G. (2018). *CrystEngComm* **20**, 3891–3897.
- Lü, X. Q., Jiang, J. J., zur Loye, H. C., Kang, B. S. & Su, C. Y. (2005a). *Inorg. Chem.* **44**, 1810–1817.
- Lü, X. Q., Zhang, L., Chen, C. L., Su, C. Y. & Kang, B. S. (2005b). *Inorg. Chim. Acta* **358**, 1771–1776.
- Sheldrick, G. M. (2015a). *Acta Cryst.* **A71**, 3–8.
- Sheldrick, G. M. (2015b). *Acta Cryst.* **C71**, 3–8.
- Spackman, P. R., Turner, M. J., McKinnon, J. J., Wolff, S. K., Grimwood, D. J., Jayatilaka, D. & Spackman, M. A. (2021). *J. Appl. Cryst.* **54**, 1006–1011.
- Yan, B., Ma, R., Chu, Z., Ding, L. Q., Long, Y., Chen, L. L., Lü, X. Q. & Bao, F. (2010). *J. Inorg. Organomet. Polym.* **20**, 809–815.

supporting information

Acta Cryst. (2026). E82, 854-857 [https://doi.org/10.1107/S2056989026006110]

Synthesis and structure of a 1:1 cocrystal of *N,N'*-bis(pyridin-3-ylmethyl)-pyromellitic diimide and naphthalene-2,6-dicarboxylic acid

Luccile Mbonzhe and Eustina Batisai

Computing details

N,N'-Bis(pyridin-3-ylmethyl)pyromellitic diimide–naphthalene-2,6-dicarboxylic acid (1/1)

Crystal data

$C_{22}H_{14}N_4O_4 \cdot C_{12}H_8O_4$

$M_r = 614.55$

Triclinic, $P\bar{1}$

$a = 6.9314$ (2) Å

$b = 8.3554$ (3) Å

$c = 12.5463$ (4) Å

$\alpha = 79.716$ (1)°

$\beta = 80.977$ (1)°

$\gamma = 74.432$ (1)°

$V = 684.15$ (4) Å³

$Z = 1$

$F(000) = 318$

$D_x = 1.492$ Mg m⁻³

Mo $K\alpha$ radiation, $\lambda = 0.71073$ Å

Cell parameters from 9965 reflections

$\theta = 2.6$ – 28.3 °

$\mu = 0.11$ mm⁻¹

$T = 130$ K

Block, yellow

$0.28 \times 0.17 \times 0.13$ mm

Data collection

BRUKER D8 QUEST

diffractometer

Radiation source: sealed tube

Detector resolution: 7.39 pixels mm⁻¹

ω scans

Absorption correction: multi-scan

(SADABS; Krause *et al.*, 2015)

$T_{\min} = 0.650$, $T_{\max} = 0.746$

23721 measured reflections

3391 independent reflections

3048 reflections with $I > 2\sigma(I)$

$R_{\text{int}} = 0.040$

$\theta_{\max} = 28.3$ °, $\theta_{\min} = 2.6$ °

$h = -9 \rightarrow 8$

$k = -11 \rightarrow 11$

$l = -16 \rightarrow 16$

Refinement

Refinement on F^2

Least-squares matrix: full

$R[F^2 > 2\sigma(F^2)] = 0.039$

$wR(F^2) = 0.107$

$S = 1.10$

3391 reflections

211 parameters

1 restraint

Primary atom site location: dual

Hydrogen site location: mixed

H atoms treated by a mixture of independent

and constrained refinement

$w = 1/[\sigma^2(F_o^2) + (0.0491P)^2 + 0.3031P]$

where $P = (F_o^2 + 2F_c^2)/3$

$(\Delta/\sigma)_{\max} < 0.001$

$\Delta\rho_{\max} = 0.36$ e Å⁻³

$\Delta\rho_{\min} = -0.28$ e Å⁻³

Special details

Geometry. All esds (except the esd in the dihedral angle between two l.s. planes) are estimated using the full covariance matrix. The cell esds are taken into account individually in the estimation of esds in distances, angles and torsion angles; correlations between esds in cell parameters are only used when they are defined by crystal symmetry. An approximate (isotropic) treatment of cell esds is used for estimating esds involving l.s. planes.

Fractional atomic coordinates and isotropic or equivalent isotropic displacement parameters (\AA^2)

	<i>x</i>	<i>y</i>	<i>z</i>	$U_{\text{iso}}^*/U_{\text{eq}}$
O1	0.94933 (14)	0.56834 (11)	0.61477 (7)	0.0239 (2)
H1	0.887 (2)	0.6401 (17)	0.5555 (9)	0.036*
O18	0.26446 (15)	0.92395 (11)	0.09152 (7)	0.0272 (2)
O23	0.50906 (14)	0.42909 (11)	0.30621 (7)	0.0243 (2)
O3	0.94674 (14)	0.81605 (11)	0.66050 (7)	0.0233 (2)
N9	0.74937 (16)	0.76234 (12)	0.46376 (8)	0.0198 (2)
N16	0.36780 (14)	0.69532 (12)	0.22228 (8)	0.0174 (2)
C7	1.08872 (17)	0.31773 (14)	0.92125 (9)	0.0174 (2)
H7	1.139624	0.199353	0.934264	0.021*
C8	1.06660 (16)	0.39725 (14)	0.81661 (9)	0.0171 (2)
H8	1.098256	0.333481	0.757836	0.021*
C4	0.99645 (16)	0.57470 (14)	0.79612 (9)	0.0161 (2)
C2	0.96390 (16)	0.66531 (14)	0.68329 (9)	0.0175 (2)
C14	0.59674 (18)	0.72163 (14)	0.43038 (9)	0.0199 (2)
H14	0.570054	0.615645	0.459367	0.024*
C13	0.47578 (17)	0.82771 (14)	0.35519 (9)	0.0170 (2)
C15	0.30468 (17)	0.77764 (14)	0.31994 (9)	0.0188 (2)
H15B	0.252472	0.700467	0.379958	0.023*
H15A	0.193824	0.878866	0.305142	0.023*
C17	0.33909 (17)	0.77633 (14)	0.11648 (9)	0.0182 (2)
C19	0.41928 (16)	0.64345 (13)	0.04451 (9)	0.0161 (2)
C20	0.42361 (17)	0.65689 (14)	−0.06757 (9)	0.0173 (2)
H20A	0.373241	0.760065	−0.111895	0.021*
C21	0.49260 (16)	0.49242 (13)	0.10978 (9)	0.0161 (2)
C10	0.78669 (18)	0.91129 (15)	0.42350 (10)	0.0203 (2)
H10	0.893561	0.940894	0.448094	0.024*
C11	0.67585 (19)	1.02447 (15)	0.34729 (11)	0.0239 (3)
H11	0.707520	1.128836	0.318970	0.029*
C12	0.51751 (18)	0.98197 (15)	0.31325 (10)	0.0221 (2)
H12	0.438083	1.057794	0.261594	0.027*
C22	0.46261 (16)	0.52553 (14)	0.22495 (9)	0.0171 (2)
C5	0.94801 (16)	0.66816 (14)	0.88063 (9)	0.0168 (2)
H5	0.903446	0.786937	0.865789	0.020*
C6	0.96400 (16)	0.58878 (13)	0.98974 (9)	0.0157 (2)

Atomic displacement parameters (\AA^2)

	U^{11}	U^{22}	U^{33}	U^{12}	U^{13}	U^{23}
O1	0.0342 (5)	0.0199 (4)	0.0182 (4)	−0.0031 (3)	−0.0112 (3)	−0.0029 (3)

O18	0.0375 (5)	0.0159 (4)	0.0253 (4)	0.0007 (4)	-0.0065 (4)	-0.0037 (3)
O23	0.0314 (5)	0.0212 (4)	0.0178 (4)	-0.0035 (3)	-0.0039 (3)	-0.0003 (3)
O3	0.0315 (5)	0.0200 (4)	0.0205 (4)	-0.0099 (3)	-0.0075 (3)	0.0012 (3)
N9	0.0262 (5)	0.0188 (5)	0.0152 (4)	-0.0048 (4)	-0.0051 (4)	-0.0029 (3)
N16	0.0195 (4)	0.0170 (4)	0.0165 (4)	-0.0040 (3)	-0.0025 (3)	-0.0044 (3)
C7	0.0182 (5)	0.0158 (5)	0.0183 (5)	-0.0031 (4)	-0.0025 (4)	-0.0036 (4)
C8	0.0175 (5)	0.0184 (5)	0.0160 (5)	-0.0041 (4)	-0.0015 (4)	-0.0045 (4)
C4	0.0147 (5)	0.0187 (5)	0.0152 (5)	-0.0047 (4)	-0.0029 (4)	-0.0015 (4)
C2	0.0156 (5)	0.0204 (5)	0.0168 (5)	-0.0048 (4)	-0.0027 (4)	-0.0021 (4)
C14	0.0280 (6)	0.0173 (5)	0.0154 (5)	-0.0077 (4)	-0.0035 (4)	-0.0013 (4)
C13	0.0189 (5)	0.0170 (5)	0.0149 (5)	-0.0033 (4)	-0.0004 (4)	-0.0050 (4)
C15	0.0188 (5)	0.0206 (5)	0.0179 (5)	-0.0047 (4)	-0.0003 (4)	-0.0067 (4)
C17	0.0194 (5)	0.0171 (5)	0.0187 (5)	-0.0043 (4)	-0.0030 (4)	-0.0039 (4)
C19	0.0160 (5)	0.0143 (5)	0.0184 (5)	-0.0041 (4)	-0.0024 (4)	-0.0026 (4)
C20	0.0188 (5)	0.0145 (5)	0.0182 (5)	-0.0038 (4)	-0.0035 (4)	-0.0008 (4)
C21	0.0162 (5)	0.0162 (5)	0.0166 (5)	-0.0053 (4)	-0.0026 (4)	-0.0015 (4)
C10	0.0217 (5)	0.0205 (5)	0.0203 (5)	-0.0062 (4)	-0.0028 (4)	-0.0051 (4)
C11	0.0266 (6)	0.0168 (5)	0.0289 (6)	-0.0074 (4)	-0.0060 (5)	0.0008 (4)
C12	0.0229 (6)	0.0177 (5)	0.0243 (6)	-0.0032 (4)	-0.0059 (4)	0.0007 (4)
C22	0.0169 (5)	0.0167 (5)	0.0183 (5)	-0.0049 (4)	-0.0020 (4)	-0.0032 (4)
C5	0.0173 (5)	0.0161 (5)	0.0171 (5)	-0.0041 (4)	-0.0033 (4)	-0.0014 (4)
C6	0.0141 (5)	0.0167 (5)	0.0167 (5)	-0.0036 (4)	-0.0023 (4)	-0.0030 (4)

Geometric parameters (Å, °)

O1—C2	1.3135 (14)	C13—C12	1.3900 (16)
O1—H1	0.9501 (10)	C13—C15	1.5080 (15)
O18—C17	1.2073 (14)	C15—H15B	0.9900
O23—C22	1.2094 (14)	C15—H15A	0.9900
O3—C2	1.2182 (14)	C17—C19	1.4921 (15)
N9—C10	1.3335 (15)	C19—C20	1.3867 (15)
N9—C14	1.3391 (15)	C19—C21	1.3924 (15)
N16—C22	1.3911 (14)	C20—C21 ⁱⁱ	1.3872 (15)
N16—C17	1.3963 (14)	C20—H20A	0.9500
N16—C15	1.4619 (14)	C21—C22	1.4917 (15)
C7—C8	1.3732 (15)	C10—C11	1.3843 (17)
C7—C6 ⁱ	1.4216 (15)	C10—H10	0.9500
C7—H7	0.9500	C11—C12	1.3870 (17)
C8—C4	1.4201 (15)	C11—H11	0.9500
C8—H8	0.9500	C12—H12	0.9500
C4—C5	1.3748 (15)	C5—C6	1.4179 (15)
C4—C2	1.5013 (15)	C5—H5	0.9500
C14—C13	1.3889 (16)	C6—C6 ⁱ	1.422 (2)
C14—H14	0.9500		
C2—O1—H1	106.8 (11)	O18—C17—C19	128.73 (11)
C10—N9—C14	118.72 (10)	N16—C17—C19	105.69 (9)
C22—N16—C17	112.33 (9)	C20—C19—C21	122.87 (10)

C22—N16—C15	123.31 (9)	C20—C19—C17	129.04 (10)
C17—N16—C15	124.37 (9)	C21—C19—C17	108.09 (10)
C8—C7—C6 ⁱ	120.49 (10)	C19—C20—C21 ⁱⁱ	114.62 (10)
C8—C7—H7	119.8	C19—C20—H20A	122.7
C6 ⁱ —C7—H7	119.8	C21 ⁱⁱ —C20—H20A	122.7
C7—C8—C4	120.09 (10)	C20 ⁱⁱ —C21—C19	122.52 (10)
C7—C8—H8	120.0	C20 ⁱⁱ —C21—C22	129.54 (10)
C4—C8—H8	120.0	C19—C21—C22	107.95 (9)
C5—C4—C8	120.49 (10)	N9—C10—C11	122.60 (11)
C5—C4—C2	117.92 (10)	N9—C10—H10	118.7
C8—C4—C2	121.54 (10)	C11—C10—H10	118.7
O3—C2—O1	124.33 (10)	C10—C11—C12	118.46 (11)
O3—C2—C4	121.82 (10)	C10—C11—H11	120.8
O1—C2—C4	113.81 (10)	C12—C11—H11	120.8
N9—C14—C13	122.82 (11)	C11—C12—C13	119.57 (11)
N9—C14—H14	118.6	C11—C12—H12	120.2
C13—C14—H14	118.6	C13—C12—H12	120.2
C14—C13—C12	117.83 (11)	O23—C22—N16	125.12 (10)
C14—C13—C15	121.26 (10)	O23—C22—C21	128.96 (10)
C12—C13—C15	120.91 (10)	N16—C22—C21	105.93 (9)
N16—C15—C13	111.95 (9)	C4—C5—C6	120.56 (10)
N16—C15—H15B	109.2	C4—C5—H5	119.7
C13—C15—H15B	109.2	C6—C5—H5	119.7
N16—C15—H15A	109.2	C5—C6—C7 ⁱ	121.66 (10)
C13—C15—H15A	109.2	C5—C6—C6 ⁱ	118.99 (12)
H15B—C15—H15A	107.9	C7 ⁱ —C6—C6 ⁱ	119.35 (12)
O18—C17—N16	125.59 (11)		
C6 ⁱ —C7—C8—C4	1.93 (17)	C17—C19—C20—C21 ⁱⁱ	-179.30 (11)
C7—C8—C4—C5	-0.73 (17)	C20—C19—C21—C20 ⁱⁱ	0.13 (19)
C7—C8—C4—C2	-177.93 (10)	C17—C19—C21—C20 ⁱⁱ	179.46 (10)
C5—C4—C2—O3	18.94 (16)	C20—C19—C21—C22	-179.81 (10)
C8—C4—C2—O3	-163.79 (11)	C17—C19—C21—C22	-0.48 (12)
C5—C4—C2—O1	-158.88 (10)	C14—N9—C10—C11	-1.02 (18)
C8—C4—C2—O1	18.39 (15)	N9—C10—C11—C12	1.23 (19)
C10—N9—C14—C13	0.25 (17)	C10—C11—C12—C13	-0.65 (18)
N9—C14—C13—C12	0.28 (17)	C14—C13—C12—C11	-0.06 (17)
N9—C14—C13—C15	-179.75 (10)	C15—C13—C12—C11	179.98 (11)
C22—N16—C15—C13	83.09 (13)	C17—N16—C22—O23	177.96 (11)
C17—N16—C15—C13	-97.45 (12)	C15—N16—C22—O23	-2.52 (18)
C14—C13—C15—N16	-92.23 (12)	C17—N16—C22—C21	-1.83 (12)
C12—C13—C15—N16	87.73 (13)	C15—N16—C22—C21	177.69 (9)
C22—N16—C17—O18	-178.33 (12)	C20 ⁱⁱ —C21—C22—O23	1.7 (2)
C15—N16—C17—O18	2.15 (19)	C19—C21—C22—O23	-178.40 (12)
C22—N16—C17—C19	1.54 (12)	C20 ⁱⁱ —C21—C22—N16	-178.55 (11)
C15—N16—C17—C19	-177.97 (10)	C19—C21—C22—N16	1.39 (12)
O18—C17—C19—C20	-1.4 (2)	C8—C4—C5—C6	-1.07 (16)
N16—C17—C19—C20	178.69 (11)	C2—C4—C5—C6	176.22 (10)

O18—C17—C19—C21	179.28 (12)	C4—C5—C6—C7 ⁱ	-178.81 (10)
N16—C17—C19—C21	-0.59 (12)	C4—C5—C6—C6 ⁱ	1.64 (19)
C21—C19—C20—C21 ⁱⁱ	-0.12 (18)		

Symmetry codes: (i) $-x+2, -y+1, -z+2$; (ii) $-x+1, -y+1, -z$.

Hydrogen-bond geometry ($\text{\AA}, ^\circ$)

<i>D</i> —H \cdots <i>A</i>	<i>D</i> —H	H \cdots <i>A</i>	<i>D</i> \cdots <i>A</i>	<i>D</i> —H \cdots <i>A</i>
O1—H1 \cdots N9	0.95 (1)	1.64 (1)	2.5806 (13)	172 (2)
C15—H15A \cdots O3 ⁱⁱⁱ	0.99	2.56	3.4073 (14)	143
C11—H11 \cdots O23 ^{iv}	0.95	2.51	3.2402 (15)	134
C10—H10 \cdots O3 ^v	0.95	2.64	3.2414 (15)	122
C11—H11 \cdots O3 ^v	0.95	2.62	3.2207 (15)	122

Symmetry codes: (iii) $-x+1, -y+2, -z+1$; (iv) $x, y+1, z$; (v) $-x+2, -y+2, -z+1$.